Impact of vaccinations, boosters and lockdowns on COVID-19 waves in French Polynesia

Lloyd AC Chapman[1,2], Maite Aubry[3], Noémie Maset[4], Timothy W Russell[1], Edward S Knock[5], John A Lees[5,6], Henri-Pierre Mallet[4], Van-Mai Cao-Lormeau[3], and Adam J Kucharski[1,3]

[1]Centre for Mathematical Modelling of Infectious Diseases, London School of Hygiene and Tropical Medicine
[2]Department of Mathematics and Statistics, Lancaster University
[3]Laboratoire de recherche sur les infections virales émergentes, Institut Louis Malardé, Tahiti, French Polynesia
[4]Cellule Epi-surveillance Plateforme COVID-19, Tahiti, French Polynesia
[5]MRC Centre for Global Infectious Disease Analysis, Imperial College London
[6]European Molecular Biology Laboratory, European Bioinformatics Institute EMBL-EBI

Abstract

Estimation of the impact of vaccination and non-pharmaceutical interventions (NPIs) on COVID-19 incidence is complicated by several factors, including the successive emergence of SARS-CoV-2 variants of concern and changing population immunity resulting from vaccination and previous infection. We developed an age-structured multi-strain COVID-19 transmission model framework that could estimate the impact of vaccination and NPIs while accounting for these factors. We applied this approach to French Polynesia, which unlike many countries experienced multiple large COVID-19 waves from multiple variants over the course of the pandemic, interspersed with periods of elimination. We estimated that the vaccination programme averted 54.3% (95% CI 54.0-54.6%) of the 6840 hospitalisations and 60.2% (95% CI 59.9–60.5%) of the 1280 hospital deaths that would have occurred in a baseline scenario without any vaccination up to May 2022. Vaccination also averted an estimated 28.4% (95% CI 28.2-28.7%) of 193,000 symptomatic cases in the baseline scenario. We estimated the booster campaign contributed 3.4%, 2.9% and 3.3% to overall reductions in cases, hospitalisations and hospital deaths respectively. Our results suggested that removing, or altering the timings of, the lockdowns during the first two waves had non-linear effects on overall incidence owing to the resulting effect on accumulation of population immunity. Our estimates of vaccination and booster impact differ from those for other countries due to differences in age structure, previous exposure levels and timing of variant introduction relative to vaccination, emphasising the importance of detailed analysis that accounts for these factors.

Introduction

Since late 2020, multiple new severe acute respiratory coronavirus 2 (SARS-CoV-2) variants have emerged and spread globally, of which the major variant groups (Alpha, Beta, Gamma, Delta, and Omicron) have shown substantially different levels of transmissibility, severity and/or immune escape. At the same time, first- and second-dose vaccinations and booster doses against COVID-19 have been rolled out in many countries around the world, drastically changing population-level immunity and reducing incidence of severe COVID-19 outcomes [1–6]. In this context, estimating the impact of vaccination and non-pharmaceutical interventions (NPIs) on COVID-19 incidence is challenging, because it is necessary to account for: different variant properties, a complicated and ever-changing immune landscape from vaccination and previous infection, and the timing of variant emergence relative to vaccination roll-out and previous epidemic waves. Most existing modelling analyses of vaccination impact have not explicitly accounted for different variant

properties and the array of different levels and types of immunity that now exist [1–4, 7], and thus may no longer offer the best available evidence. Here we develop a framework that explicitly includes these different factors and apply it to COVID-19 epidemic waves in French Polynesia.

As of early 2023, French Polynesia has experienced five waves of COVID-19 cases. The first, caused by the wild-type virus, started in August 2020 and peaked in early November 2020. Transmission then declined with the introduction of strict control measures, including a ban on gatherings in public places, mandatory mask wearing and a curfew, until cases reached very low levels again in February 2021. This low level of cases – driven by imports – was then maintained until mid-2021 when the rollout of the 1st and 2nd vaccine doses occurred. Following the introduction of the Delta variant in June 2021, the country experienced a second larger and sharper wave of cases, hospitalisations and deaths, with cases peaking in mid-August 2021. A lockdown was implemented with the establishment of a curfew and confinement at home on the main island groups (the Windward and Leeward Islands) in August 2021, and cases declined quickly back to low levels in November 2021. The arrival of the Omicron BA.1/BA.2 variants in late December 2021 led to a relatively large third wave of cases, but fewer hospitalisations and deaths than in the previous waves, which coincided with the rollout of first booster doses. During the first trimester of 2022, incoming travellers were screened for infection at the border using PCR (polymerase chain reaction)/antigen tests. The third wave had largely subsided by April 2022. French Polynesia experienced a fourth wave of cases mainly caused by the Omicron BA.5 and BA.4 variants between June and September 2022 [8] and a fifth wave mainly caused by the BQ.1.1 Omicron sub-variant in November and December 2022. During the third, fourth and fifth waves, no strong NPIs (curfews or case isolation) were implemented.

To understand how immunity and control measures shaped observed dynamics in French Polynesia, we fit an age-structured multi-strain COVID-19 transmission model to reported case, hospitalisation and death data up to May 2022, as well as data from two seroprevalence surveys conducted in February 2021 and November-December 2021. We then use the fitted model to estimate the impact of NPIs and vaccination on numbers of COVID-19 cases, hospitalisations and deaths, and to estimate the immune status of the French Polynesian population.

Results

Model fit

The fit of the model to the overall numbers of cases, hospitalisations, and deaths between July 2020 and May 2022 is shown in Figure 1, and the fit of the model to the age-stratified numbers of confirmed cases, hospitalisations and hospital deaths is shown in Figure S5 and S4, and to the age-stratified data from the seroprevalence surveys in Figure S6. The model reproduces the overall patterns in the data, although it does not fully capture the flatness of the first wave of hospitalisations and hospital deaths, underestimates deaths among 60+ year-olds in the second wave, and overestimates hospitalisations in the third wave. The estimated number of symptomatic cases over time corresponds closely to the numbers of confirmed cases during the three waves, with a fitted reporting factor of 0.55 (95% CI 0.53–0.57) (Figure 1).

Impact of NPIs

We estimate the counterfactual impact that the lockdowns during the first two COVID-19 waves had on the numbers of symptomatic cases, hospitalisations and deaths in each wave and overall by simulating the model without the estimated reductions in the transmission rate corresponding to the lockdown periods in the first and second waves (Figure S9). We run 500 simulations with parameter values drawn from the posterior distribution of the parameters from the model fitting and compare the numbers of symptomatic cases, hospitalisations and hospital deaths to those in simulations with the estimated reductions in the transmission rate with lockdowns, to account for uncertainty in the estimated parameter values. This gives the results shown in Table 1 and Figure 2.

The estimated overall numbers of symptomatic cases, hospitalisations and hospital deaths from fitting the model to the observed data up to May 2022 are 138,000 (95% CI 137,000–139,000), 3120 (95% CI 300–3230) and 510 (95% CI 493–526) respectively. We estimated that removing the lockdowns in both the first and second waves would have had a non-linear effect on dynamics, and – assuming everything else had remained

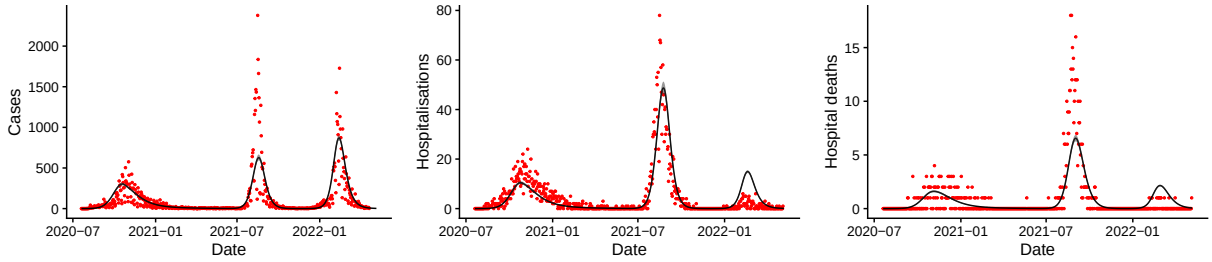

Figure 1: Fit of the model to the observed total numbers of confirmed cases, hospitalisations and hospital deaths over time. Red dots show observed counts, black line and grey shaded area show median and 95% CI of simulations of the fitted model, i.e. the uncertainty in the expected number of each outcome in the model. Note that this does not include uncertainty in the reporting process and that there is a strong day-of-the-week effect in the reporting that accounts for the much of the dispersion in the data. Note different scales on vertical axes.

the same – would have led to fewer hospitalisations and hospital deaths overall (768 (95% CI 729–816) and 107 (95% CI 101–115) fewer, respectively) but a slightly higher number of symptomatic cases (600 (95% CI 100–1000) more). This scenario assumes that patients hospitalised during the first wave would have been managed the same (in terms of treatment and ICU admission) had the number of hospitalisations in the first wave been nearly twice as high. The non-linear effect on overall incidence is due to the first wave of infections being much larger, resulting in greater build up of immunity in the population prior to the introduction of the more severe Delta variant, and therefore a much smaller second wave of cases, hospitalisations and deaths (with 31,000 (95% CI 30,000–32,300) fewer cases, 1430 (1370-1510) fewer hospitalisations, and 230 (95% CI 220-242) fewer deaths). The impact on the third wave would have been relatively limited due to the effects on the first two waves approximately cancelling each other out in terms of cumulative infections, and the immune escape properties of the Omicron BA.1/BA.2 variants reducing the influence of immunity from previous infection. Overall hospitalisations and deaths would have decreased, despite the increase in overall cases, as the reduction in cases in the second wave would have been slightly greater than the increase in cases in the first wave and there are more hospitalisations and deaths per case in the second wave than the first due to the greater severity of the Delta variant.

We also considered the counterfactual impact that changing the timings of the lockdowns during the first two waves would have had on incidence in each wave and overall (Supplementary Material §1.3). We estimated that starting the first and second lockdowns 2 weeks earlier or later would have had relatively little impact on overall numbers of cases, hospitalisations and deaths due to a similar non-linear cancellation effect between infections in the first and second waves as for removing the lockdowns.

Table 1: Median (95% CI) estimated total numbers of symptomatic cases, hospitalisations and hospital deaths in different COVID-19 waves in French Polynesia up to May 2022 for different counterfactual scenarios of lockdowns, vaccination and booster rollout.

Counterfactual	Cases (thousands)				Hospitalisations				Hospital deaths			
	Wave 1	Wave 2	Wave 3	Total	Wave 1	Wave 2	Wave 3	Total	Wave 1	Wave 2	Wave 3	Total
No change	40 (38.6–41.2)	40.7 (39.8–41.6)	57.1 (56.7–57.5)	138 (137–139)	783 (747–819)	1770 (1710–1840)	566 (547–586)	3120 (3020–3230)	132 (126–138)	282 (271–293)	95.9 (92.7–99.3)	510 (49[illegible]526)
No lockdowns	68.6 (68–69.2)	9.7 (9.18–10.2)	60.1 (59.6–60.6)	138 (137–139)	1420 (1370–1470)	340 (317–365)	595 (574–616)	2350 (2280–2440)	249 (241–258)	51.1 (47.4–55.1)	102 (98.4–106)	402 (38[illegible]417)
No vaccination	40.4 (39–41.7)	62.4 (61.5–63.4)	89.7 (89.5–90)	193 (192–193)	794 (757–830)	4300 (4140–4450)	1750 (1690–1810)	6840 (6610–7070)	134 (127–140)	824 (795–853)	321 (311–332)	1280 (1240–1320)
No boosters	40 (38.6–41.2)	40.7 (39.9–41.6)	61.9 (61.6–62.3)	143 (142–144)	783 (747–819)	1770 (1710–1840)	658 (635–681)	3210 (3110–3320)	132 (126–138)	282 (271–293)	113 (109–117)	527 (5[illegible]543)

Wave 1 = 20th July 2020 to 30th June 2021
Wave 2 = 1st July 2021 to 30th November 2021
Wave 3 = 1st December 2021 to 6th May 2022.

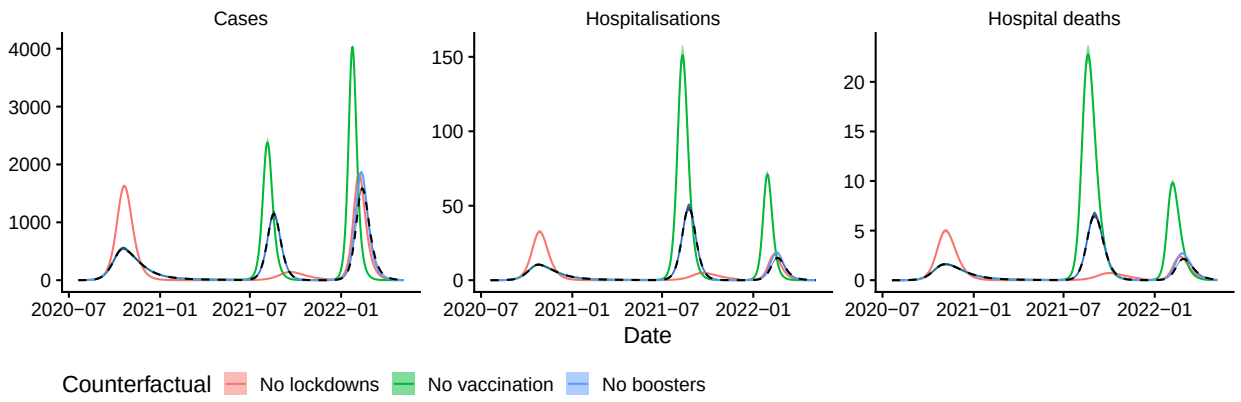

Figure 2: Impact of lockdowns, vaccination programme and booster programme on numbers of COVID-19 symptomatic cases, hospitalisations, and hospital deaths. Solid lines and shaded areas show medians and 95% CI of 500 simulations of the model. Dashed black line and grey shaded area show median and 95% CI of simulations of the fitted model.

Impact of vaccination

The counterfactual impact of vaccination on numbers of hospitalisations and deaths during each wave and overall was estimated by simulating the fitted model without any vaccination, and comparing the numbers of hospitalisations and deaths to those in simulations with the actual vaccination rollout (Table 1 and Figure 2). The vaccination programme is estimated to have averted 54,700 (95% CI 54,500-54,900) symptomatic cases, 3710 (95% CI 3570–3860) hospitalisations and 770 (95% CI 740–799) hospital deaths overall, with nearly all of these being averted during the second and third waves, since vaccination did not start until mid-January 2021 when the first wave had largely subsided.

Under our base case assumption about the rate at which booster protection wanes, the booster campaign is estimated to have had a moderate impact on the overall numbers of cases, hospitalisations and deaths, reducing them by 4800 (95% CI 4800–4900), 92 (95% CI 89-95) and 17 (95% CI 17–18) respectively (Table 1 and Figure 2). However, these estimates are highly sensitive to the assumed booster waning rate. With a less conservative assumption about the rate at which individuals lose all protection from boosters, the estimated reductions in cases, hospitalisations and deaths are 8100 (95% CI 8000–8200), 213 (95% CI 202–221), and 44 (95% CI 43–46) respectively (see §1.4 in the Supplementary Material for further details).

Immune status of the population

The breakdown of the inferred immune status of the population over time and by age is shown in Figure 3. The three waves of cases are visible where the proportion recovered from infection increases sharply in October 2020, August 2021, and February 2022. Based on the model, most infections in the Delta wave were among unvaccinated uninfected individuals, while in the Omicron BA.1/BA.2 wave just under a half were among individuals with 2nd dose protection or waned 2nd dose protection, either with or without immunity from previous infection. The model also suggests that in May 2022 a very high proportion (89.4% (95% CI 89.1–89.5%)) of the population possessed either natural or hybrid (natural + vaccine-induced) immunity, and only 2.6% the population were fully susceptible. Table 2 shows the full breakdown of the estimated immune status of the population in May 2022. As expected, given prioritisation of older individuals in the vaccine and booster rollouts, the proportion of the population that had only natural immunity in May 2022 decreased with increasing age, from over 95% among 0-9-year-olds to just over 20% among 70+ year-olds, while the proportion with hybrid immunity from infection and a booster dose increased with age from 0% among 0-9 year-olds to over 30% among 50+ year-olds.

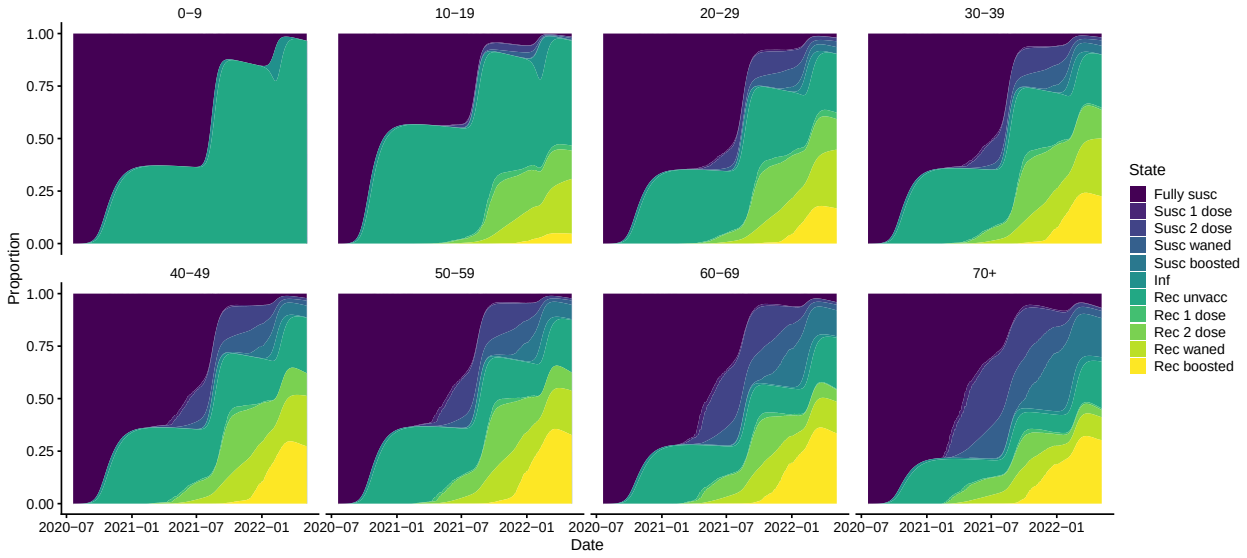

Figure 3: Inferred immune status of the population over time by age group. Coloured bands show median estimates from 1000 simulations of the fitted model. Note that the fully susceptible category includes individuals whose immunity from infection or vaccination has waned. Susc = suscceptible, Inf = infected, Rec = recovered.

Table 2: Estimated immune status of the overall population on 6th May 2022

State	Number, median (95% CI)	Percentage, median (95% CI)
Fully susceptible	7190 (7070 – 7310)	2.56 (2.52 – 2.60)
Susceptible 1 dose	182 (179 – 186)	0.065 (0.064 – 0.066)
Susceptible 2 dose	2780 (2710 – 2850)	0.99 (0.97 – 1.01)
Susceptible waned	5470 (5350 – 5600)	1.95 (1.90 – 2.00)
Susceptible boosted	13500 (13200 – 13800)	4.81 (4.71 – 4.92)
Infected	813 (789 – 839)	0.29 (0.28 – 0.30)
Recovered unvacc	111000 (111000 – 111000)	39.5 (39.4 – 39.5)
Recovered 1 dose	2950 (2950 – 2950)	1.05 (1.05 – 1.05)
Recovered 2 dose	26800 (26800 – 26900)	9.55 (9.53 – 9.57)
Recovered waned	56900 (56800 – 57100)	20.3 (20.2 – 20.3)
Recovered boosted	53400 (53100 – 53700)	19.0 (18.9 – 19.1)

Discussion

We have used an age-structured multi-strain SARS-CoV-2 transmission model that accounts for different levels of protection from vaccination and previous infection, waning of immunity, and different variant properties (transmissibility and severity) to estimate the impact of vaccination and non-pharmaceutical interventions on incidence of cases and severe outcomes in the first three waves of COVID-19 in French Polynesia. We have estimated impact through comparison with counterfactual scenarios, including no lockdowns, earlier/later introduction of lockdowns, no vaccination and no boosters.

The first two vaccine doses had a large estimated impact on incidence in the Delta and Omicron BA.1/BA.2 waves, averting over 50,000 symptomatic cases, 3500 hospitalisations and nearly 800 deaths up to May 2022 compared to a counterfactual scenario of no vaccination. Our estimate for the number of deaths averted through vaccination in French Polynesia is much lower than that from a recent study estimating the global impact of vaccination at a country level [1], which estimated that 2120 (95% CI 1740–2570) deaths had been averted up to 8th December 2021. There are a number of reasons for this difference. The main source of the discrepancy is that our estimate is derived from fitting to reported daily hospital deaths

(of which there were 552 between July 2020 and May 2022 with recorded date of death), whereas that from [1] is based on an estimate of weekly excess mortality from a boosted regression tree model of global excess deaths [9], which gave an estimated total of 920 (95% CI 790-1200) excess deaths between December 2020 and December 2021. We chose to fit to hospital deaths rather than all deaths (hospital deaths + community deaths) as they are less sensitive to context bias. We assumed quality of patient care was the same during the different waves and that the risk of death given hospitalisation remained constant. However, deaths in the community are likely to have varied to a greater extent over the different waves, as there was considerable fear and distrust of hospitalisation during the Delta wave when hospitals reached capacity, and less distrust in healthcare in the first wave and less fear of severe outcomes during the Omicron BA.1/BA.2 wave. Given extensive follow-up of hospitalised cases it is likely that under-reporting of hospital deaths in French Polynesia was not as high as elsewhere [10]. We also fit to multiple other direct data streams (including reported cases, hospitalisations and seroprevalence), whereas Watson et al. [1] only fit to estimated excess deaths, so our estimate may be more robust. A further small source of difference is that we estimate *hospital* deaths averted not *all* deaths averted, so the ∼5% of deaths in the community averted through vaccination are not included in our estimates.

We estimated that the booster campaign had less of an impact on the BA.1/BA.2 wave than the first two doses had on the Delta wave, in both absolute and proportional terms, despite similar numbers of infections in the BA.1/BA.2 wave as in the Delta wave. Although this may seem surprising, e.g. when compared with the estimated impact of the booster rollout in the UK [11], the estimated small effect size is influenced by a combination of factors. These include the already high level of natural/hybrid immunity in the population from previous infection and/or vaccination (Figure 3), the relatively low booster coverage during the wave (<35% of the overall population and only >50% in individuals ≥50 years) (Figure 4), and the lower severity of the BA.1/BA.2 variants.

Our results suggest that – all other things being equal – changing lockdown dates during the first two waves by two weeks would have had limited impact on overall numbers of cases, hospitalisations and deaths. This is because starting the first lockdown either earlier or later would have led to more infections prior to the second wave and thus been compensated for by a smaller second wave due to greater population immunity, and moving the second lockdown earlier or later would have had only a small impact on incidence due to its relatively limited estimated effect on the transmission rate (Figure S9). In addition, incidence in the Omicron BA.1/BA.2 wave would have been largely unaffected due to the limited net effect of changes in the lockdowns on incidence in the first two waves.

We also estimated the composition of immunity from infection and vaccination in the population in May 2022. We estimated that 97% of the population had some form of immunity, predominantly either natural or hybrid immunity (as opposed to only vaccine-induced immunity). From this we would expect that infection incidence (and therefore hospitalisation and death incidence) after May 2022 would have remained low without the advent of new variants with high levels of immune escape against Omicron BA.1/BA.2, which has been the case, with the BA.5 wave being relatively small in terms of detected cases, hospitalisations and deaths [12, 13]. Given that the rollout of 2nd booster doses to those aged over 60 years began in April 2022 we would expect incidence of infections and severe outcomes to remain low for some time if no new immune escape variants are introduced.

There are some limitations to the analysis we have presented (see the Supplementary Material for an extended discussion). We make the simplifying assumptions that mixing between age groups is homogeneous for the whole French Polynesian population, despite the fact that the population is spread over many islands in five archipelagos, and that the seroprevalence estimates from the sero-surveys on the main islands of Tahiti and Moorea were representative of the seroprevalence on all the islands. However, ∼75% of the population resides on the main islands of Tahiti and Moorea (and ∼69% on Tahiti), so these assumptions are not unreasonable. We may underestimate the impact of the vaccination programme as we estimate cases, hospitalisations and deaths averted from reported hospital deaths, which are considerably lower than estimates of all-cause mortality and excess mortality [9, 14], and do not account for increased death rates among hospitalised cases and in the community when hospitals reached capacity during the Delta wave. The third wave was caused by a mixture of the Omicron BA.1 and BA.2 sublineages and there is evidence that the BA.2 variant is more transmissible than the BA.1 variant [15–18], but we do not distinguish between these subvariants when modelling the third wave, which may lead to some underestimation of the impact of the booster programme.

Nevertheless, the framework we have developed provides a means of estimating the impact of vaccination and NPIs on COVID-19 incidence while accounting for the complex immune landscape that has developed over the course of the pandemic from myriad different infection and vaccination histories at an individual level. In particular, several different data streams can be incorporated in the inference to provide more robust estimates of key unobserved processes. As a result, the framework could be useful for analysing other countries' data to estimate vaccination and NPI impact.

Methods

Data

Multiple data streams are used in the fitting of the model. Anonymised line lists of confirmed cases and hospitalisations compiled by the Ministry of Health of French Polynesia with testing date and admission date, and date of death for those that died, and 10-year age group were aggregated into age-stratified time series of daily cases, hospitalisations and hospital deaths. Only 493 out of 74986 confirmed cases (0.66%) were missing their age group, so these cases were treated as unreported cases, since under-reporting of cases is accounted for in the model fitting (see *Confirmed cases*). As testing dates were missing for a large number of cases early in the first wave and cases were numbered approximately sequentially by testing date in the surveillance system, we imputed the missing dates as being between the testing dates of the nearest numbered cases with recorded testing dates. Data from two sero-surveys, the first conducted by Cellule Epi-surveillance COVID and the Health Department of French Polynesia in February 2021, the second by Institut Louis Malardé in November-December 2021, was also used. This data is described in detail in [8] and summarised in Table 3. Briefly, in February 2021, 463 unvaccinated adults aged 18-88 years on the islands of Tahiti and Moorea were randomly selected and tested for anti-SARS-CoV-2 immunoglobulin type G (IgG) antibodies with the Siemens SARS-CoV-2 IgG (sCOVG) test. Overall, 88 (19.0%, 95% CI 15.5–22.9%) individuals had detectable IgG antibodies. In November-December 2021, 673 randomly selected individuals aged $\geq$18 years on Tahiti were tested for antibodies against the SARS-CoV-2 N antigen (i.e. for evidence of past infection) with the Roche Elecsys anti-SARS-CoV-2 assay, and 388 (57.7%, 95% CI 53.8–61.4%) were positive. For the purposes of the modelling, we assume that the seroprevalence in the 20-29 years age group in the model is the same as that in the 18-29 years age group in the data. We use data on the population of French Polynesia by year of age in 2020 from the UN World Population Prospects [19] (for which the total population was estimated to be 280,904) aggregated into 10-year age groups for the age group populations in the model.

We use data on daily numbers of first, second and booster doses administered by age group (12-17, 18-29, 30-39, 40-49, 50-59, 60-69, 70+ years) collected by the Ministry of Health of French Polynesia to determine the numbers of individuals moving between the different vaccination strata in the model. Since the model is stratified into 10-year age groups, we split the doses in the 18-29 years age group in the data into the 10-19 and 20-29 age groups in the model according to population proportion (the proportions of 18-29 year-olds that are 18-19 and 20-29 years old). Upon division by the population in each age group, this gives the vaccination coverage by age and dose shown in Figure 4.

Model

We developed a deterministic age-structured multi-strain SEIR-type model of COVID-19 transmission with stratification by vaccination status (Figure 5). The model is stratified into 8 age groups (0-9, 10-19, 20-29, 30-39, 40-49, 50-59, 60-69, 70+ years), and by 5 vaccination levels representing no vaccination, protection from 1 dose, protection from 2 doses, waned protection from the 2nd dose and protection from a booster dose.

In the model, individuals enter an exposed state upon infection with a particular variant, from where an age-dependent proportion develop symptoms after a presymptomatic infection period, while the rest progress to asymptomatic infection. Presymptomatic, symptomatic and asymptomatic individuals are all assumed to be infectious, though asymptomatic individuals less so. Most symptomatic individuals and all asymptomatic individuals recover naturally, but some symptomatic individuals develop severe disease that can lead to hospitalisation. A proportion of these individuals die from the disease while in hospital or at

Table 3: Seroprevalence in February 2021 and November-December 2021

Age group (years)	Feb 2021 survey			Nov-Dec 2021 survey		
	Participants (n)	Seropositive (n)	Seroprevalence (%) (95% CI)	Participants (n)	Seropositive (n)	Seroprevalence (%) (95% CI)
18-29	60	12	20 (10.8–32.3)	169	103	60.9 (53.2–68.3)
30-39	90	15	16.7 (9.6–26)	163	105	64.4 (56.6–71.7)
40-49	78	17	21.8 (13.2–32.6)	92	54	58.7 (47.9–68.9)
50-59	95	17	17.9 (10.8–27.1)	79	48	60.8 (49.1–71.6)
60-69	93	18	19.4 (11.9–28.9)	113	56	49.6 (40–59.1)
70+	47	9	19.1 (9.1–33.3)	57	22	38.6 (26–52.4)
Total	463	88	19.0 (15.5–22.9)	673	388	57.7 (53.8–61.4)

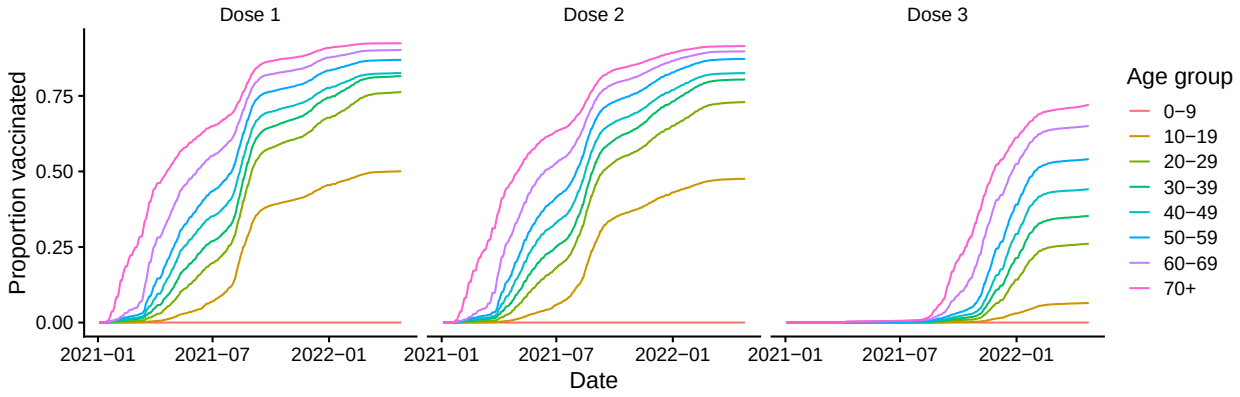

Figure 4: Vaccination coverage by vaccine dose. Dose 3 = booster dose.

home, while the remainder recover following treatment. Infected individuals are assumed to cease being infectious upon recovery. Once recovered from infection individuals have immunity against reinfection with the same variant that wanes over time, but only partial immunity against infection with a different variant.

Individuals in the susceptible, exposed, presymptomatic, asymptomatic and recovered states can be vaccinated, providing them with increased levels of protection against infection, hospitalisation and death. The different vaccination strata and their associated levels of protection are shown in Tables 4 and 5.

The model is further stratified to account for different histories of infection with two different variants: the latest variant to have emerged and the previously dominant variant. Individuals can have been infected by only the previous variant, only the current variant, or the previous variant and the current variant (in either order), giving 4 possible infection histories. Once a new variant emerges the information stored in the strata for the two variants is combined into the stratum for the first variant, and the information for the new variant added to the second stratum.

Here we ignore transmission of the Alpha variant, as although Alpha was detected among travellers and a small number of local cases in early 2021 through variant screening (Table 10), transmission of Alpha remained localised and never became fully established. We therefore only explicitly model the introduction and spread of the Delta and Omicron variants. We also do not distinguish between the Omicron BA.1 and BA.2 sublineages, and model the introduction of Omicron and its sublineages as a single new variant.

Naturally-acquired immunity is assumed to wane slowly — individuals who have been infected are assumed to return to being susceptible to infection with the same variant after an exponentially distributed period with a mean of 6 years [11]. Immunity between SARS-CoV-2 variants is assumed to be asymmetric, with infection with later variants conferring stronger protection against infection with earlier variants than vice versa (see *Force of infection* and Table 6 for details). Changes in population-level serological status with seroconversion and seroreversion following infection are modelled with a "parallel flow".

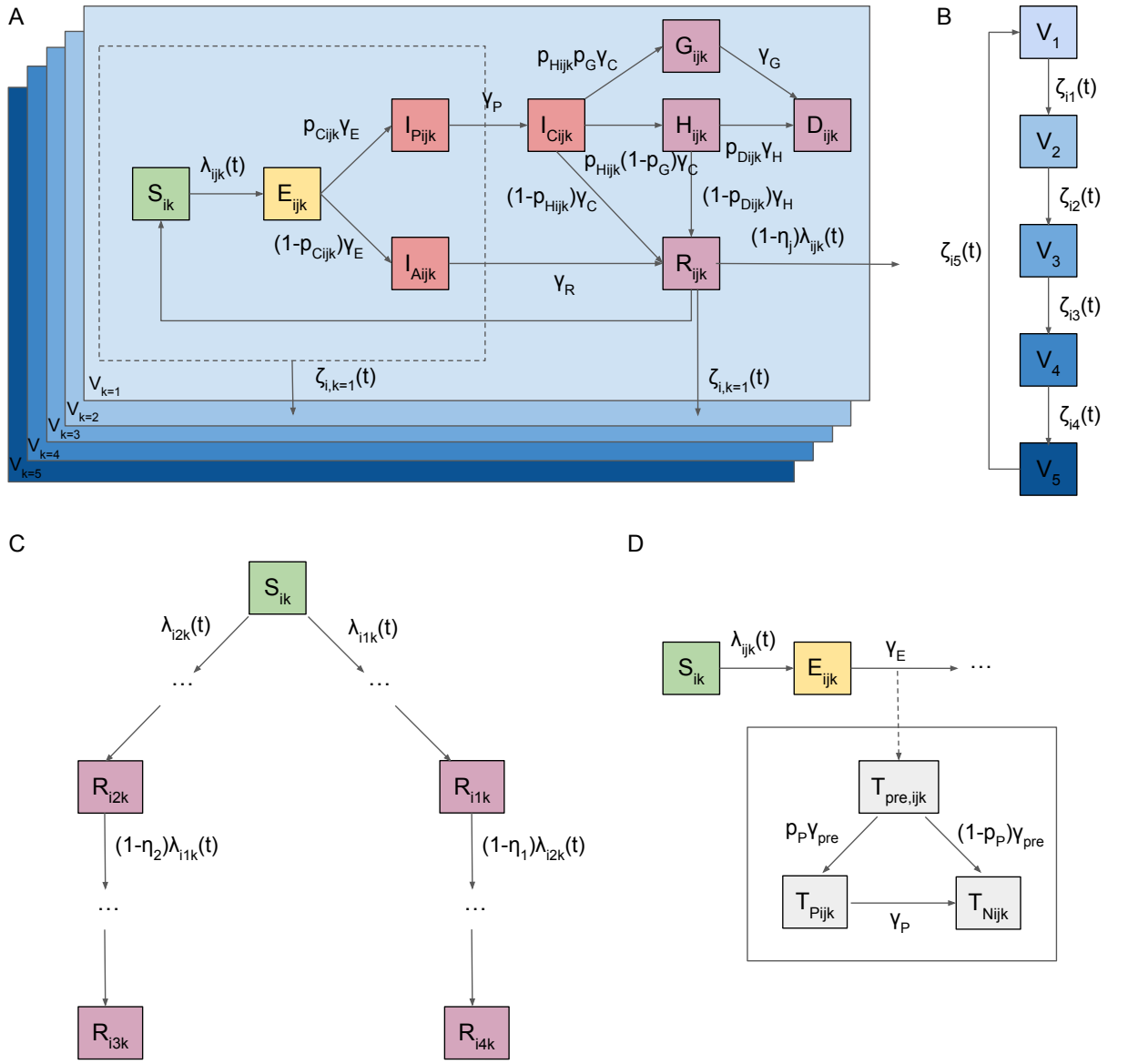

Figure 5: Model flow diagram. (A) SEIR-type transmission model structure with infectious states shown in red and different vaccination strata shown in blue. Individuals in states inside dashed box and recovered from infection (R_{ijk}) can move between vaccination strata upon vaccination. (B) Vaccination strata flow diagram. (C) Multi-strain model structure showing possible infection with first variant or second variant, or first then second, or second then first. (D) Seropositivity model structure with "parallel flow" to transmission model flow. Transition rates between states are shown on arrows. All symbols are defined in the Model equations section and Tables 4, 6 and 8, and further details of the model structure are provided below. Subscripts denote the age group ($i \in \{0-9, 10-19, 20-29, 30-39, 40-49, 50-59, 60-69, 70+\}$ years), variant ($j \in \{1, 2, 3, 4\}$, where $j = 3$ represents infection by variant 1 followed by infection by variant 2, and $j = 4$ vice versa), and vaccination stratum ($k \in \{1, 2, 3, 4\}$).

Demographic processes such as birth, natural death and migration are ignored in the model (i.e. the population is assumed to remain constant in the absence of deaths from COVID-19). These processes occur at a much slower rate than transmission processes and are therefore assumed to have a negligible impact on the transmission dynamics over the timescales modelled.

Vaccination

Details of the five vaccination strata in the model are shown in Table 4. Unvaccinated individuals move out of the first vaccination stratum at a rate determined by the roll-out of the 1st vaccine dose, with an assumed delay of 28 days for immunity from the 1st dose to develop. Likewise, movement into the second dose vaccination stratum is determined by the roll-out of the second dose, with a delay of 14 days for the dose to take full effect. Only non-symptomatic and non-hospitalised individuals, i.e. individuals in the S, E, I_A, I_P and R states in the model, can be vaccinated. Protection from the second vaccine dose is assumed to wane over an exponentially distributed period, with a mean duration of 6 months, after which individuals pass into a 'waned' vaccine state, with lower levels of protection. They either remain in this state or receive a booster vaccination and move into a 'boosted' vaccination state, with higher levels of protection. Protection from the booster dose is assumed to wane slowly such that individuals eventually return to being fully susceptible.

In common with other transmission modelling studies [11, 20], we model vaccine protection against five different outcomes:

1. infection, with effectiveness e^{inf}
2. symptomatic infection given infection, $e^{sympt|inf}$
3. severe disease given symptomatic infection, $e^{SD|sympt}$
4. death given severe disease, $e^{death|SD}$
5. onward transmission if infected, e^{ins}

Vaccine effectiveness against symptomatic infection, severe disease and death are conditional on previous outcomes and depend on overall vaccine effectiveness against infection, symptomatic infection, severe disease and death (e^{inf}, e^{sympt}, e^{SD} and e^{death}) as follows:

$$
\begin{aligned}
e^{sympt|inf} &= \frac{e^{sympt} - e^{inf}}{1 - e^{inf}} \\
e^{SD|sympt} &= \frac{e^{SD} - e^{sympt}}{(1 - e^{inf})(1 - e^{sympt|inf})} \\
&= \frac{e^{SD} - e^{sympt}}{1 - e^{sympt}} \\
e^{death|SD} &= \frac{e^{death} - e^{SD}}{(1 - e^{inf})(1 - e^{sympt|inf})(1 - e^{SD|sympt})} \\
&= \frac{e^{death} - e^{SD}}{1 - e^{SD}}
\end{aligned}
$$

Estimates for e^{inf}, e^{sympt}, e^{SD} and e^{death} for different vaccination strata and variants taken from [11] are provided in Table 5 (see [11] for information on sources of these estimates). As the over 90% of the doses given in French Polynesia were of the Pfizer-BioNTech vaccine, we use effectiveness values for that vaccine for all doses given. We also assume that vaccine effectiveness is the same across all age groups.

Waning immunity

The model accounts for waning of natural and vaccine-induced immunity as described in the previous sections. We assume the same rate of waning of natural and vaccine-induced immunity for all age groups and virus variants. When immunity from previous infection or booster vaccination wanes, individuals return to being fully susceptible, so immunity against different outcomes (infection, symptomatic infection, hospitalisation and death) is assumed to wane at the same rate. We note that this is a strong simplifying assumption as there is evidence to suggest that immunity against infection wanes more quickly than immunity against severe outcomes [22], and that immunity against infection and severe outcomes wanes faster for Omicron BA.1 than Delta [21]. As there is no data that provides a direct measure of the rate of loss of all protection from vaccination, we use the rate of waning of protection against hospitalisation as a proxy for the rate at which

Table 4: Vaccination strata in the model

Vaccination stratum	Dose number	Vaccine effectiveness	Mean duration	References
V_1	0	None	Determined by vaccine roll-out	
V_2	1	Full 1st dose effectiveness (28 days after 1st dose)	Determined by vaccine roll-out	
V_3	2	Full 2nd dose effectiveness (14 days after 2nd dose)	6 months	[20]
V_4	2	Waned 2nd dose effectiveness	Determined by vaccine roll-out	
V_5	3	Booster effectiveness	$-80/(365\log(0.818)) = 1.1$ years, $-140/(365\log(0.923)) = 4.8$ years	[11, 21] (sensitivity)

Table 5: Vaccine effectiveness against different infection outcomes for different variants and levels of vaccination

Outcome	Variant	Vaccine effectiveness (%)				
		Symbol	1 dose	2 doses	2 doses + waned	2 doses + booster
Infection	Wild-type & Alpha		70	85	48	95
	Delta	e^{inf}	62	80	45	91.4
	Omicron		34.2	44.1	24.8	65.9
Symptoms	Wild-type & Alpha		70	90	51	95
	Delta	e^{sympt}	62	81	61	91.9
	Omicron		34.2	46.9	46.7	67.6
Severe disease	Wild-type & Alpha		85	95	65	99
	Delta	e^{SD}	92	96	84.2	99
	Omicron		76.7	83.7	67.6	93.3
Death	Wild-type & Alpha		85	95	66	99
	Delta	e^{death}	92	96	84.2	99
	Omicron		76.7	83.7	67.6	93.3
Infectiousness if infected	Wild-type & Alpha	e^{ins}	47	47	30	37
	Delta		24	37	24	37
	Omicron		24	37	24	37
Delay to effect			28 days	14 days	Immediate	Immediate

Vaccine effectiveness estimates for Pfizer-BioNTech vaccine from [11].
*Assumed based on relative effectiveness against different outcomes for Delta due to limited evidence on booster effectiveness against wild-type and Alpha variants.

individuals return to being fully susceptible following booster vaccination. Whilst a reasonable assumption, this may still be overly conservative, so we also conduct a sensitivity analysis with different values of the waning rate from the literature. Although we do not model variant-specific vaccine waning rates, we use estimates of the change in protection against hospitalisation over time following booster administration for Omicron BA.1 [21] for the booster waning rate in the analysis in the main text, since the booster campaign in French Polynesia coincided with the Omicron BA.1/BA.2 wave, and compare this to a lower waning rate assumed by Barnard et al. [11] in their model with a similar structure (Table 6). See §1.4 for results of the sensitivity analysis.

Parallel flow for serological status

So that we can fit to the data from the sero-surveys we include a "parallel flow" of compartments for serological status in addition to those for infection status and clinical progression (Figure 5). We fit to the data on prevalence of seropositivity against the N antigen on the SARS-CoV-2 virus according to the Roche Elecsys anti-SARS-CoV-2 assay, as this tests only for positivity resulting from infection. After a pre-conversion period (T_{pre}), individuals either seroconvert (T_P) with probability p_P or not (T_N). Those that do seroconvert eventually serorevert (to T_N) after an exponentially distributed time with mean 6.6 years [23].

Model equations

Force of infection

The relative susceptibility to infection with variant j of a susceptible individual in age group i in vaccination stratum k is given by:

$$\chi_{ijk} = 1 - e^{inf}_{ijk},$$

where e^{inf}_{ijk} is the vaccine effectiveness against infection with variant j in vaccination stratum $k \in \{1, 2, 3, 4, 5\}$ (see Table 5), and $\chi_{ij1} = 1, \forall i, j$ (i.e. there is no protection in unvaccinated individuals). The index j denotes individuals' infection histories, covering primary infection with one variant ($j \in \{1, 2\}$) and superinfection (infection with one variant followed by infection with another) ($j \in \{3, 4\}$) as follows:

$$j = \begin{cases} 1, & \text{if individuals have only been infected by 1st variant} \\ 2, & \text{if individuals have only been infected by 2nd variant} \\ 3, & \text{if individuals infected by 1st variant followed by 2nd variant } (1 \to 2) \\ 4, & \text{if individuals infected by 2nd variant followed by 1st variant } (2 \to 1). \end{cases}$$

The relative infectiousness of an individual in age group i and vaccination stratum k infected with variant j compared with an unvaccinated individual infected with the wild-type virus is given by:

$$\xi_{ijk} = \sigma_j(1 - e^{ins}_{ijk})$$

where $\xi_{i11} = 1, \forall i$, and σ_j is the relative transmissibility of variant j compared to the wild-type variant (and we assume $\sigma_1 = \sigma_4$ and $\sigma_2 = \sigma_3$).

The infectiousness-weighted number of infectious individuals for variant j in age group i and vaccination stratum k on day t is given by

$$\Theta_{ijk}(t) = \xi_{ijk}\left(\theta_A I_{A,ijk} + I_{P,ijk} + I_{C,ijk}\right).$$

where θ_A is the relative infectiousness of an asymptomatic infected individual compared to a symptomatic individual in the same vaccination stratum infected with the same variant.

With these definitions, the force of infection on a susceptible individual in age group i and vaccination stratum k from variant j on day t is:

$$\lambda_{ijk}(t) = \begin{cases} \chi_{i1k} \sum_{i'} m_{ii'}(t) \sum_k (\Theta_{i',1,k}(t) + \Theta_{i',2\to1,k}(t)), & \text{if } j = 1, \\ \chi_{i2k} \sum_{i'} m_{ii'}(t) \sum_k (\Theta_{i',2,k}(t) + \Theta_{i',1\to2,k}(t)), & \text{if } j = 2. \end{cases}$$

where $m_{ii'}(t) = \beta(t)c_{ii'}$ is the symmetric time-varying person-to-person transmission rate from age group i' to age group i, composed of the time-varying transmission rate $\beta(t)$ and the symmetric person-to-person contact matrix $c_{ii'}$ between age groups. The contact matrix $c_{ii'}$ was parameterised using estimates of contact rates between 5-year age groups for France from [24] averaged over 10-year age groups in the model with population data for French Polynesia by year of age from the UN World Population Prospects [19]. Social contact data for France was used due to the absence of estimates for French Polynesia and the fact that French Polynesia is a French territory.

The total force of infection on a susceptible individual in age group i and vaccination stratum k is then the sum of the variant-specific forces of infection:

$$\Lambda_{ik}(t) = \sum_{j=1}^{2} \lambda_{ijk}(t).$$

Cross-immunity between variants is modelled via partial immunity to infection with the other variant following infection with one variant, such that the force of infection on an individual in age group i and vaccination stratum k recovered from infection with variant j is:

$$\begin{cases} (1-\eta_j)\lambda_{i,3-j,k}(t), & \text{if } j \in \{1,2\} \\ 0, & \text{if } j \in \{3,4\} \end{cases}$$

where η_j is the cross-immunity of variant j with the other variant.

The time-varying transmission rate, $\beta(t)$, represents temporal changes in the overall contact rates in the population due to changes in restrictions and behaviour. We assume that $\beta(t)$ is piecewise linear with 5 changepoints corresponding to changes in alert levels and the imposition of island-wide restrictions such as curfews (Table 9 and Figure S9):

$$\beta(t) = \begin{cases} \beta_1, & \text{if } t \leq t_1 \\ \frac{t_i - t}{t_i - t_{i-1}}\beta_{i-1} + \frac{t - t_{i-1}}{t_i - t_{i-1}}\beta_i, & \text{if } t_{i-1} < t \leq t_i, i \in \{2,\ldots,5\} \\ \beta_5, & \text{if } t > t_5. \end{cases} \quad (1)$$

Natural history parameters

Movement between model compartments is determined by parameters p_X, defining the probability of progressing to compartment X, and rate parameters γ_X, defining the time individuals stay in compartment X, which can vary with age group (i), variant (j) and vaccination status (k). Values of these parameters are given in Tables 6 and 7 and information on how they are calculated is given below.

The probability of developing symptoms given infection is

$$p_{Cijk} = (1 - e_{ijk}^{sympt|inf})p_{Ci}$$

where p_{Ci} is the age-dependent probability of developing symptoms given infection for unvaccinated individuals.

The probability that an individual develops severe disease requiring hospitalisation given that they are symptomatically infected is

$$p_{Hijk} = (1 - e_{ijk}^{SD|sympt})\omega_{Hj}p_{Hi}$$

where p_{Hi} is the age-dependent probability of developing severe disease given symptomatic infection for unvaccinated individuals and ω_{Hj} is the variant-dependent relative risk of severe disease. p_{Hi} is defined as:

$$p_{Hi} = \psi_{Hi}p_{Hmax}$$

where p_{Hmax} is the maximum probability of hospitalisation across all age groups and $\psi_{Hi} = 1$ for the group corresponding to the maximum.

The probability that a hospitalised individual will die is

$$p_{Dijk} = e_{ijk}^{death|SD}\omega_{Dj}\psi_{Di}p_{Dmax}$$

where ω_{Dj} is the variant-dependent relative risk of death, p_{Dmax} is the maximum probability of death given hospitalisation for unvaccinated individuals, and ψ_{Di} is the age-dependent relative risk of death for unvaccinated individuals (such that $\psi_{Di} = 1$ for the age group for which the probability of death is p_{Dmax}).

The probability that an individual dies in the community given that they have severe disease is

$$p_{Gijk} = e_{ijk}^{death|SD}\omega_{Dj}p_G$$

where p_G is the probability of death in the community given severe disease for unvaccinated individuals.

Table 6: Fixed model parameters

Parameter	Description	Stratum, j	Value	Reference
γ_E	Rate of progression from latent infection		0.5	[25, 26]
γ_A	Rate of progression from asymptomatic infection		0.2	[25]
γ_P	Rate of progression from presymptomatic infection		0.4	[25]
γ_C	Rate progression from symptomatic infection		0.4	[25]
γ_G	Rate of progression from severe illness to death in the community		0.3	[26]
γ_H	Rate of progression from severe illness to death in hospital		0.10	[26]
γ_{pre}	Rate of seroconversion following infection		0.077	[20]
γ_P	Rate of seroreversion following seroconversion	Roche N assay	0.0004	[23]
γ_R	Rate of waning of natural immunity following infection		0.00046	[11]
η_j	Cross immunity to infection with new variant following infection with variant j	Wild type/Alpha against infection with Delta	0.95	[11, 20]
		Delta against infection with wild type/Alpha	1	[20]
		Delta against infection with Omicron	0.55	[11]
		Omicron against infection with Delta	1	[11]
p_G	Probability of death in the community given severe disease		0.053	Calculated from data on total hospitalisations and community deaths
$p_{D\,max}$	Maximum probability of death given hospitalisation		0.316	[27]
θ_A	Relative infectiousness of asymptomatic individuals		0.5	[25]
	Number of initial infections in seed age group (30-39-years-old)		10	Assumed
	Initial seeding pattern of `initial_seed_size` from t_0		1	Assumed
σ_j	Relative transmissibility of variant j vs wild type	Delta	2.8	[11]
		Omicron	3.5	[11]
	Number of infections of variant j seeded in 0-39 age group	Delta	10	Assumed
		Omicron	10	Assumed
	Seeding pattern of `strain_seed_size` infections from t_{Delta}	Delta	1	Assumed
		Omicron	1	Assumed
$\omega_{C\,j}$	Relative probability of symptomatic infection for variant j vs wild type	Delta	1	Assumed
		Omicron	1	Assumed
$\omega_{H\,j}$	Relative probability of hospitalisation for variant j vs wild type	Delta	1.6*1.85 = 2.96	[28, 29]
		Omicron	0.555	[30]
$\omega_{D\,j}$	Relative probability of death for variant j vs wild type	Delta	1	Assumed
		Omicron	1	Assumed
$\zeta_{ik}(t)$	Rate of movement from vaccination group k to vaccination group k+1 in age group i	Unvaccinated	Determined by vaccination schedule	
		Vaccinated with 1 dose	Determined by vaccination schedule	
		Vaccinated with 2 doses	0.0055	[11, 20]
		Vaccinated & waned	Determined by vaccination schedule	
		Boosted	0.0025, 0.00057	[11, 21] (sensitivity analysis)
p_P	Probability of seroconversion following infection		0.85	[31]
p_{sens}	Sensitivity of serological test		1	Assumed such that proportion of infected individuals who develop a detectable antibody response (= proportion that develop response * test sensitivity) is 0.85
p_{spec}	Specifity of serological test		0.99	[31]
κ_H	Shape parameter for negative binomial hospitalisation observation process		20	Assumed
κ_D	Shape parameter for negative binomial hospital death observation process		20	Assumed
κ_{cases}	Shape parameter for negative binomial confirmed case observation process		2	Assumed

Table 7: Fixed age-dependent model parameters

Age group (years)	Probability of symptomatic infection for age group i [32] p_{C_i}	Relative probability of hospitalisation given symptomatic infection for age group i [27] ψ_{H_i}	Relative probability of death given hospitalisation for age group i [27] ψ_{D_i}
0-9	0.29	0.009	0.019
10-19	0.207	0.064	0.035
20-29	0.268	0.108	0.06
30-39	0.328	0.112	0.104
40-49	0.398	0.192	0.206
50-59	0.486	0.314	0.399
60-69	0.631	0.389	0.665
70+	0.691	1	1

Table 8: Definitions of model compartments

Compartment	Definition
S_{ik}	Number of susceptible individuals
E_{ijk}	Number of exposed (latently infected) individuals
I_{Aijk}	Number of asymptomatic infected individuals
I_{Pijk}	Number of presymptomatic infected individuals
I_{Cijk}	Number of symptomatic (clinical) infected individuals
H_{ijk}	Number of hospitalised individuals
G_{ijk}	Number of severely diseased individuals who will die at home
D_{ijk}	Number who have died from COVID-19
R_{ijk}	Number of recovered individuals
$T_{pre_{ijk}}$	Number of individuals pre-seropositive against N antigen
T_{Pijk}	Number of individuals seropositive against N antigen
T_{Nijk}	Number of individuals seronegative against N antigen

See Figure 5 for a flow diagram of the model. All symbols denote the numbers of individuals in each compartment at time t, but the dependence on t has been dropped in the notation for convenience. i denotes the age group, j the variant, and k the vaccination stratum.

Compartmental model equations

The compartmental model is a deterministic approximation to a stochastic age-structured multi-strain SEIR-type transmission model in which draws from random variables are replaced by their expected values (using the deterministic mode of the `dust` R package). This may have lower accuracy than an ODE formulation and solver, but we expect that the error is minimal based on the model fits. The model compartments are defined in Table 8. For completeness we provide the equations for the stochastic model here, and note that the stochastic version of the model can be fitted and run by setting the option `deterministic <- F` in the code.

The compartments in the model are updated according to the following equations:

$$S_{ik}(t+dt) = S_{ik}(t) - \sum_{j=1}^{2} nSE_{ijk} + nSV_{i,k-1} - nSV_{ik} + \sum_{j=1}^{2} nRS_{ijk} \tag{2}$$

$$E_{ijk}(t+dt) = E_{ijk}(t) + nSE_{ijk} + \mathbb{1}_{j>2}\, nRE_{i,j-2,k} - nEI_{A_{ijk}} - nEI_{P_{ijk}} + nEV_{ij,k-1} - nEV_{ijk} \tag{3}$$

$$I_{Aijk}(t+dt) = I_{Aijk}(t) + nEI_{Aijk} - nI_AR_{ijk} + nI_AV_{ij,k-1} - nI_AV_{ijk} \tag{4}$$

$$I_{Pijk}(t+dt) = I_{Pijk}(t) + nEI_{Pijk} - nI_PI_{Cijk} + nI_PV_{ij,k-1} - nI_PV_{ijk} \tag{5}$$

$$I_{Cijk}(t+dt) = I_{Cijk}(t) + nI_PI_{Cijk} - nI_CR_{ijk} - nI_CH_{ijk} - nI_CG_{ijk} \tag{6}$$

$$H_{ijk}(t+dt) = H_{ijk}(t) + nI_CH_{ijk} - nHR_{ijk} - nHD_{ijk} \tag{7}$$

$$G_{ijk}(t+dt) = G_{ijk}(t) + nI_CG_{ijk} - nGD_{ijk} \tag{8}$$

$$D_{ijk}(t+dt) = D_{ijk}(t) + nHD_{ijk} + nGD_{ijk} \tag{9}$$

$$R_{ijk}(t+dt) = R_{ijk}(t) + nI_AR_{ijk} + nI_CR_{ijk} + nHR_{ijk} - nRS_{ijk} - \mathbb{1}_{j\leq 2}\, nRE_{ijk} + nRV_{ij,k-1} - nRV_{ijk} \tag{10}$$

$$T_{pre_{ijk}}(t+dt) = T_{pre_{ijk}}(t) + nEI_{Aijk} + nEI_{Pijk} - nT_{pre}T_{P_{ijk}} - nT_{pre}T_{N_{ijk}} \tag{11}$$

$$T_{Pijk}(t+dt) = T_{Pijk}(t) + nT_{pre}T_{P_{ijk}} - nT_PT_{N_{ijk}} \tag{12}$$

$$T_{Nijk}(t+dt) = T_{Nijk}(t) + nT_{pre}T_{N_{ijk}} + nT_PT_{N_{ijk}} \tag{13}$$

where nXY_{ijk} is the number of individuals in age group i and vaccination stratum k infected with variant j (if they are in an infection state) moving from state X to state Y at time t (and $nXY_{ij0} = nXY_{ij5}$, and we have dropped the dependence on t from the notation for convenience); dt is the model time step, chosen to be 0.25 days; and $\mathbb{1}_x$ is the indicator function for condition x.

The flows between states are determined as follows:

$$p_{SE_{ijk}} = \left(1 - e^{-\Lambda_{ik}(t)dt}\right) \frac{\lambda_{ijk}(t)}{\Lambda_{ik}(t)}, \quad j \in \{1, 2\} \tag{14}$$

$$p_{SV_{ik}} = e^{-\Lambda_{ik}(t)dt} \left(1 - e^{-\zeta_{ik}(t)dt}\right) \tag{15}$$

$$(nSE_{i1k}, nSE_{i2k}, nSV_{ik}, nSS_{ik}) \sim \text{Mult}(S_{ik}(t), p_{SE_{i1k}}, p_{SE_{i2k}}, p_{SV_{ik}}, 1 - \sum_j p_{SE_{ijk}} - p_{SV_{ik}}) \tag{16}$$

$$p_{EI_{A_{ijk}}} = (1 - p_{C_{ijk}}) \left(1 - e^{-\gamma_E dt}\right) \tag{17}$$

$$p_{EI_{P_{ijk}}} = p_{C_{ijk}} \left(1 - e^{-\gamma_E dt}\right) \tag{18}$$

$$p_{EV_{ijk}} = e^{-\gamma_E dt} \left(1 - e^{-\zeta_{ik}(t)dt}\right) \tag{19}$$

$$(nEI_{A_{ijk}}, nEI_{P_{ijk}}, nEV_{ijk}, nEE_{ijk}) \sim \text{Mult}(E_{ijk}(t), p_{EI_{A_{ijk}}}, p_{EI_{P_{ijk}}}, 1 - \sum_{X \in I_A, I_P, V} p_{EX_{ijk}}) \tag{20}$$

$$(p_{I_A R_{ijk}}, p_{I_A V_{ijk}}) = \left(1 - e^{-\gamma_A dt}, e^{-\gamma_A dt}(1 - e^{-\zeta_{ik}(t)dt})\right) \tag{21}$$

$$(nI_A R_{ijk}, nI_A V_{ijk}, nI_A I_{A_{ijk}}) \sim \text{Mult}(I_{A_{ijk}}(t), p_{I_A R_{ijk}}, p_{I_A V_{ijk}}, 1 - p_{I_A R_{ijk}} - p_{I_A V_{ijk}}) \tag{22}$$

$$(p_{I_P I_{C_{ijk}}}, p_{I_P V_{ijk}}) \sim \left(1 - e^{-\gamma_P dt}, e^{-\gamma_P dt}(1 - e^{-\zeta_{ik}(t)dt}\right) \tag{23}$$

$$(nI_P I_{C_{ijk}}, nI_P V_{ijk}, nI_P I_{P_{ijk}}) \sim \text{Mult}(I_{P_{ijk}}(t), p_{I_P I_{C_{ijk}}}, p_{I_P V_{ijk}}, 1 - p_{I_P I_{C_{ijk}}} - p_{I_P V_{ijk}}) \tag{24}$$

$$p_{I_C H_{ijk}} = p_{H_{ijk}}(1 - p_{G_{ijk}}) \left(1 - e^{-\gamma_H dt}\right) \tag{25}$$

$$p_{I_C G_{ijk}} = p_{H_{ijk}} p_{G_{ijk}} \left(1 - e^{-\gamma_H dt}\right) \tag{26}$$

$$p_{I_C R_{ijk}} = (1 - p_{H_{ijk}}) \left(1 - e^{-\gamma_H dt}\right) \tag{27}$$

$$(nI_C H_{ijk}, nI_C G_{ijk}, nI_C R_{ijk}, nI_C I_{C_{ijk}}) \sim \text{Mult}(I_{C_{ijk}}(t), p_{I_C H_{ijk}}, p_{I_C G_{ijk}}, p_{I_C R_{ijk}}, 1 - \sum_{X \in H, G, R} p_{I_C X_{ijk}}) \tag{28}$$

$$p_{HD_{ijk}} = p_{D_{ijk}} \left(1 - e^{-\gamma_H dt}\right) \tag{29}$$

$$p_{HR_{ijk}} = (1 - p_{D_{ijk}}) \left(1 - e^{-\gamma_H dt}\right) \tag{30}$$

$$(nHD_{ijk}, nHR_{ijk}, nHH_{ijk}) \sim \text{Mult}(H_{ijk}(t), p_{HD_{ijk}}, p_{HR_{ijk}}, 1 - p_{HD_{ijk}} - p_{HR_{ijk}}) \tag{31}$$

$$nGD_{ijk} \sim \text{Bin}(G_{ijk}, 1 - e^{-\gamma_G dt}) \tag{32}$$

$$\gamma_{RE_{ijk}} = \mathbb{1}_{j \leq 2}(1 - \eta_j)\lambda_{i,3-j,k} \tag{33}$$

$$p_{RS_{ijk}} = \left(1 - e^{-(\gamma_R + \gamma_{RE_{ijk}})dt}\right) \frac{\gamma_R}{\gamma_R + \gamma_{RE_{ijk}}} \tag{34}$$

$$p_{RE_{ijk}} = \left(1 - e^{-(\gamma_R + \gamma_{RE_{ijk}})dt}\right) \frac{\gamma_{RE_{ijk}}}{\gamma_R + \gamma_{RE_{ijk}}} \tag{35}$$

$$p_{RV_{ijk}} = e^{-(\gamma_R + \gamma_{RE_{ijk}})dt} \left(1 - e^{-\zeta_{ik}(t)dt}\right) \tag{36}$$

$$(nRS_{ijk}, nRE_{ijk}, nRV_{ijk}, nRR_{ijk}) = \text{Mult}(R_{ijk}(t), p_{RS_{ijk}}, p_{RE_{ijk}}, p_{RV_{ijk}}, 1 - \sum_{X \in S, E, V} p_{RX_{ijk}}) \tag{37}$$

$$p_{T_{pre}T_{P_{ijk}}} = p_P \left(1 - e^{-\gamma_{pre} dt}\right) \tag{38}$$

$$p_{T_{pre}T_{N_{ijk}}} = (1 - p_P) \left(1 - e^{-\gamma_{pre} dt}\right) \tag{39}$$

$$(nT_{pre}T_{P_{ijk}}, nT_{pre}T_{N_{ijk}}, nT_{pre}T_{pre_{ijk}}) \sim \text{Mult}(T_{pre_{ijk}}(t), p_{T_{pre}T_{P_{ijk}}}, p_{T_{pre}T_{N_{ijk}}}, 1 - p_{T_{pre}T_{P_{ijk}}} - p_{T_{pre}T_{N_{ijk}}}) \tag{40}$$

$$nT_P T_{N_{ijk}} \sim \text{Bin}(T_{P_{ijk}}(t), 1 - e^{-\gamma_P dt}) \tag{41}$$

where nXX_{ijk} is the number of individuals in age group i and vaccination stratum k infected with variant j (if they are in an infection state) who do not move from state X at time t.

Model likelihood

The model likelihood is composed of the likelihoods for the different data streams that the model is fitted to, namely the age-stratified time series of hospitalisations, hospital deaths and confirmed cases, and the age-stratified seroprevalence data, as detailed below.

In the following, $Y \sim \text{Bin}(n, p)$ denotes that Y follows a binomial distribution with n trials and success probability p, such that

$$P(Y = y) = P_{\text{Bin}}(y|n, p) = \binom{n}{y} p^y (1-p)^{n-y}.$$

and the mean and variance of Y are np and $np(1-p)$ respectively. $Y \sim \text{NegBin}(m, \kappa)$ denotes that Y follows a negative binomial distribution with mean m and shape parameter κ, such that

$$P(Y = y) = P_{\text{NegBin}}(y|m, \kappa) = \frac{\Gamma(\kappa + y)}{y!\Gamma(\kappa)} \left(\frac{\kappa}{\kappa + m}\right)^{\kappa} \left(\frac{m}{\kappa + m}\right)^{y}$$

where $\Gamma(k)$ is the gamma function, and the variance of Y is $m + m^2/\kappa$.

Hospitalisations

We assume that the observed number of hospitalisations in each age group at time t, $Y_{Hi}(t)$, is distributed according to a negative binomial distribution

$$Y_{Hi}(t) \sim \text{NegBin}(X_{Hi}(t), \kappa_H)$$

with mean

$$X_{Hi}(t) = \sum_j \sum_k n I_C H_{ijk}$$

where the shape parameter κ_H determines the overdispersion in the observation process and thus accounts for noise in the underlying data, and is taken to be 20. The contribution of the age-stratified hospitalisation data to the likelihood is therefore:

$$L_H = \prod_t \prod_i P_{\text{NegBin}}(Y_{Hi}(t)|X_{Hi}(t), \kappa_H)$$

Hospital deaths

The observed number of hospital deaths in each age group at time t is assumed to be distributed according to a negative binomial distribution:

$$Y_{Di}(t) \sim \text{NegBin}(X_{Di}(t), \kappa_D)$$

with mean

$$X_{Di}(t) = \sum_j \sum_k n H D_{ijk}$$

and overdispersion parameter κ_D, taken to be 20. The contribution of the age-stratified hospital death data to the likelihood is thus:

$$L_D = \prod_t \prod_i P_{\text{NegBin}}(Y_{Di}(t)|X_{Di}(t), \kappa_D).$$

Confirmed cases

The daily number of confirmed cases in each age group is assumed to arise as the noisy under-reported observation of a hidden underlying Markov process

$$X_{cases,i}(t) = \sum_j \sum_k n E I_{P ijk}$$

such that it follows a negative binomial distribution

$$Y_{cases,i}(t) \sim \text{NegBin}(\phi_{cases} X_{cases,i}(t), \kappa_{cases})$$

with constant reporting factor ϕ_{cases} and shape parameter κ_{cases}. The corresponding likelihood contribution is

$$L_{cases} = \prod_t \prod_i P(Y_{cases,i}(t) | X_{cases,i}(t), \kappa_{cases}, \phi_{cases}) \tag{42}$$

Seroprevalence

To fit the model to the age-stratified data from the two sero-surveys, we first calculate the number of seropositive and seronegative individuals in each age group over 20 years-of-age in the model (i.e assume the true serological status of all individuals is known):

$$\begin{aligned} X_{P\,i}(t) &= \sum_j \sum_k T_{P\,ijk}(t), \\ X_{N\,i}(t) &= N_i - \sum_j \sum_k T_{P\,ijk}(t), \quad i \in \{[20-29), \ldots, 70+\}. \end{aligned}$$

We then compare the observed number of seropositive individuals in each age group in the sero-survey, $Y_{P\,i}(t)$, with the number expected from the model based on the sample size $Y_{test,i}(t)$ and the sensitivity p_{sens} and specificity p_{spec} of the serological assay:

$$Y_{P\,i}(t) \sim \text{Bin}(Y_{test,i}(t), \omega_P(t))$$

where

$$\omega_{P\,i}(t) = \frac{p_{sens} X_{P\,i}(t) + (1 - p_{spec}) X_{N\,i}(t)}{X_{P\,i}(t) + X_{N\,i}(t)}$$

is the apparent prevalence. The likelihood contribution of the sero-survey data is:

$$L_{sero} = \prod_t \prod_i P_{\text{Bin}}(Y_{P\,i}(t) | Y_{test,i}(t), \omega_{P\,i}(t))$$

Full likelihood

The full likelihood is the product of the likelihoods for the hospitalisation, death, case and sero-survey data:

$$L = L_H L_D L_{cases} L_{sero}.$$

Prior distributions for fitted parameters

The prior distributions chosen for the fitted parameters are shown in Table 9. We use relatively informative gamma distributions for the transmission rate parameters $\beta_i \sim \text{Gamma}(k, \theta)$ $(i = 1, 2, 3, 4, 5)$:

$$f(\beta_i) = \frac{1}{\Gamma(k)\theta^k} \beta_i^{k-1} e^{-\beta_i/\theta}, \quad x > 0,$$

where $\Gamma(\cdot)$ is the Gamma function, with shape parameter $k = 4$ and scale parameter $\theta = 0.005$ to ensure that the basic reproduction number for the wild-type variant is in a sensible range. Targeted sequencing of samples from local cases and travellers to screen for new variants was performed from late December 2020 in French Polynesia (Table 10). Whilst this data is biased and so cannot be used to fit the variant proportions in the model, it can be used to constrain the introduction dates of the different variants. We use continuous uniform prior distributions for the introduction dates of the different variants, with the upper bounds of the distributions for Delta and Omicron BA.1 chosen to match the earliest date each variant was detected amongst local cases (since the variant cannot have been introduced into local circulation later than it was first detected), and the lower bounds chosen as 40 days and 12 days earlier respectively based on the earliest date

each variant was detected amongst travellers and the much higher growth rate of the Omicron BA.1 variant (Tables 9 and 10). For the wild-type variant, we assume a lower bound of 20 days prior to the first reported hospitalisation and an upper bound of 9 days later. We treat the introduction dates as continuous variables, and distribute the initial number of infections of that variant in proportion to how far between time steps the introduction date is. This helps to avoid mixing issues in the MCMC caused by treating the introduction date as a discrete variable. For the maximum probability of severe disease across all age groups and the symptomatic case reporting rate, we use completely uninformative priors, $p_{H\,max}, \phi_{cases} \sim \text{Beta}(1,1)$, where the density for $X \sim \text{Beta}(a,b)$ is:

$$f(x) = \frac{\Gamma(a+b)}{\Gamma(a)\Gamma(b)} x^{a-1}(1-x)^{b-1}, \quad x \in (0.1).$$

Table 9: Fitted model parameters prior and posterior distributions

Parameter	Description	Prior distribution	Posterior median (95% CI)
$\beta(t)$	Transmission rate (per person) on day t = YYYY-MM-DD		
β_1	2020-08-27: Moved to level 3 alert, masking became obligatory	Gamma$(4, 0.005)$	0.0327 (0.0326, 0.0329)
β_2	2020-10-24: Curfew established on the islands of Tahiti and Moorea	Gamma$(4, 0.005)$	0.0217 (0.0215, 0.022)
β_3	2021-06-01: Returned to level 1 alert, borders reopened, international flights increased	Gamma$(4, 0.005)$	0.0312 (0.0304, 0.0321)
β_4	2021-08-02: Moved to stage 4 alert, before state of health emergency and curfew instigated	Gamma$(4, 0.005)$	0.0248 (0.0241, 0.0255)
β_5	2021-11-15: Returned to level 1 alert, curfew and state of health emergency lifted	Gamma$(4, 0.005)$	0.028 (0.0278, 0.0283)
t_0	Start date of original outbreak	U[2020-07-20,2020-07-29]	2020-07-20 (2020-07-20, 2020-07-20)
t_{Delta}	Delta seeding date	U[2020-05-20,2020-06-29]	2021-06-12 (2021-06-11, 2021-06-13)
$t_{Omicron}$	Omicron seeding date	U[2021-12-01,2021-12-13]	2021-12-01 (2021-12-01, 2021-12-01)
$p_{H\,max}$	Maximum probability of severe disease requiring hospitalisation across all age groups	Beta$(1, 1)$	0.0917 (0.0884, 0.0952)
ϕ_{cases}	Symptomatic case reporting rate	Beta$(1, 1)$	0.549 (0.532, 0.565)

Table 10: Earliest dates of detection of different variants from variant screening of local cases and travellers

Variant	Earliest week detected	
	Local case	Traveller
Alpha	2021-W6 (2021-02-08)	2020-W53 (2020-12-28)
Delta	2021-W26 (2021-06-28)	2021-W23 (2021-06-07)
Omicron BA.1	2021-W50 (2021-12-13)	2021-W49 (2021-12-06)

MCMC algorithm

We use the accelerated shaping and scaling adaptive Markov Chain Monte Carlo (MCMC) algorithm of Spencer [33] to infer the values of the fitted parameters $\boldsymbol{\theta} = (\boldsymbol{\beta}, t_0, t_{Delta}, t_{Omicron}, p_{H_{max}}, \phi_{cases})$, where $\boldsymbol{\beta} = (\beta_1, \beta_2, \beta_3, \beta_4, \beta_5)$. The algorithm adaptively shapes and scales the proposal matrix to achieve more efficient mixing. We refer the reader to [33] for full details. The algorithm proceeds by repeating the following steps:

1. At the ith iteration, draw new values of the fitted parameters from a multivariate normal proposal distribution
$$\boldsymbol{\theta}_i \sim N(\boldsymbol{\theta}_{i-1}, 2.38^2 c_{i-1} \boldsymbol{\Sigma}_{i-1}/n_{\boldsymbol{\theta}})$$
where $\boldsymbol{\Sigma}_{i-1}$ is the running estimate of the covariance matrix of the posterior distribution, $n_{\boldsymbol{\theta}}$ is the dimension of the posterior density, and c_{i-1} is a scaling parameter that is tuned to achieve a desired acceptance rate (see Step 4).

2. Accept $\boldsymbol{\theta}_i$ with probability:
$$\alpha(\boldsymbol{\theta}_i, \boldsymbol{\theta}_{i-1}) = \min\left(1, \frac{L(\boldsymbol{\theta}_i)P(\boldsymbol{\theta}_i)}{L(\boldsymbol{\theta}_{i-1})P(\boldsymbol{\theta}_{i-1})}\right)$$
where $P(\boldsymbol{\theta})$ is the prior density of $\boldsymbol{\theta}$.

3. Calculate the running mean and covariance as:
if $i = 1$:
$$\overline{\boldsymbol{\theta}}_1 = \frac{1}{2}\sum_{j=0}^{1} \boldsymbol{\theta}_j$$
$$\boldsymbol{\Sigma}_1 = \frac{1}{i_0 + n_{\boldsymbol{\theta}} + 3}\left((i_0 + n_{\boldsymbol{\theta}} + 1)\boldsymbol{\Sigma}_0 + \sum_{j=0}^{1} \boldsymbol{\theta}_j \boldsymbol{\theta}_j^T - 2\overline{\boldsymbol{\theta}}_1 \overline{\boldsymbol{\theta}}_1^T\right)$$
if $f(i) = f(i-1) + 1$, where $f(i) = \lfloor \frac{i}{2} \rfloor$:
$$\overline{\boldsymbol{\theta}}_i = \overline{\boldsymbol{\theta}}_{i-1} + \frac{1}{i - f(i) + 1}(\boldsymbol{\theta}_i - \boldsymbol{\theta}_{f(i)-1})$$
$$\boldsymbol{\Sigma}_i = \boldsymbol{\Sigma}_{i-1} + \frac{1}{i - f(i) + i_0 + n_{\boldsymbol{\theta}} + 2}\left(\boldsymbol{\theta}_i \boldsymbol{\theta}_i^T - \boldsymbol{\theta}_{f(i)-1}\boldsymbol{\theta}_{f(i)-1}^T - (i - f(i) + 1)(\overline{\boldsymbol{\theta}}_{i-1}\overline{\boldsymbol{\theta}}_{i-1}^T - \overline{\boldsymbol{\theta}}_i \overline{\boldsymbol{\theta}}_i^T)\right)$$
such that the new observation replaces the oldest, and if $f(i) = f(i-1)$:
$$\overline{\boldsymbol{\theta}}_i = \frac{1}{i - f(i) + 1}((i - f(i))\overline{\boldsymbol{\theta}}_{i-1} + \boldsymbol{\theta}_i)$$
$$\boldsymbol{\Sigma}_i = \frac{1}{i - f(i) + i_0 + n_{\boldsymbol{\theta}} + 2}\left((i - f(i) + i_0 + n_{\boldsymbol{\theta}} + 1)\boldsymbol{\Sigma}_{i-1} + \boldsymbol{\theta}_i \boldsymbol{\theta}_i^T - (i - f(i))\overline{\boldsymbol{\theta}}_{i-1}\overline{\boldsymbol{\theta}}_{i-1}^T - (i - f(i) + 1)\overline{\boldsymbol{\theta}}_i \overline{\boldsymbol{\theta}}_i^T)\right)$$
such that a new observation is included, where i_0 is a constant that determines the rate at which the influence of $\boldsymbol{\Sigma}_0$ on $\boldsymbol{\Sigma}_i$ decreases.

4. Update the covariance scaling parameter c_i:
$$c_i = \max\left(c_{min}, c_{i-1}\exp\left(\frac{\delta}{i_{start} - i}(\alpha(\boldsymbol{\theta}_i, \boldsymbol{\theta}_{i-1}) - a)\right)\right)$$
where
$$\delta = \left(1 - \frac{1}{n_{\boldsymbol{\theta}}}\right)\frac{\sqrt{2\pi}\exp(A^2/2)}{2A} + \frac{1}{n_{\boldsymbol{\theta}} a(1-a)}$$
$$A = -\Phi^{-1}(a/2)$$
$$i_{start} = \frac{5}{a(1-a)}$$

with $\Phi(\cdot)$ the cumulative distribution function of the standard normal distribution, c_{min} is a minimum value for the scaling parameter (to prevent the proposal matrix being shrunk too much, which can lead to very slow mixing), and a is the target acceptance rate.

5. If $|\log(c_i) - \log(c_{start})| > \log(3)$, restart the tuning of the scaling parameter from its current value:

$$c_{start} \mapsto c_i$$
$$i_{start} \mapsto \frac{5}{a(1-a)} - i.$$

We run the above algorithm with $i_0 = 100$, $c_0 = c_{start} = 1$, $c_{min} = 1$, and a target acceptance rate of $a = 0.234$ for 50,000 iterations, with the first 5000 iterations discarded as burn-in and the remaining iterations thinned by a factor of 10. Convergence is assessed visually from parameter trace plots.

Code

The code used in this analysis uses the `odin`, `odin.dust`, `dust` and `mcstate` R packages for simulating discrete-time stochastic processes [34–37]. The model structure is similar to that of the COVID-19 transmission model in the `sircovid` R package [38], and some of the code from this package is reused. All data and code used in the analysis is available online at `https://github.com/LloydChapman/covid_multi_strain`.

Ethical approval

Secondary data analysis of routinely collected COVID-19 data from French Polynesia was approved by the London School of Hygiene and Tropical Medicine Observational Research Ethics Committee (ref 28129).

References

[1] Oliver J. Watson, Gregory Barnsley, Jaspreet Toor, Alexandra B. Hogan, Peter Winskill, and Azra C. Ghani. Global impact of the first year of covid-19 vaccination: a mathematical modelling study. *The Lancet Infectious Diseases*, 22:1293–1302, 9 2022. ISSN 14744457. doi: 10.1016/S1473-3099(22)00320-6.

[2] Valentina Marziano, Giorgio Guzzetta, Alessia Mammone, Flavia Riccardo, Piero Poletti, Filippo Trentini, Mattia Manica, Andrea Siddu, Antonino Bella, Paola Stefanelli, Patrizio Pezzotti, Marco Ajelli, Silvio Brusaferro, Giovanni Rezza, and Stefano Merler. The effect of covid-19 vaccination in italy and perspectives for living with the virus. *Nature Communications*, 12, 12 2021. ISSN 20411723. doi: 10.1038/s41467-021-27532-w.

[3] Teresa K Yamana, Marta Galanti, Sen Pei, Manuela Di Fusco, Frederick J Angulo, Mary M Moran, Farid Khan, David L Swerdlow, and Jeffrey Shaman. The impact of covid-19 vaccination in the us: averted burden of sars-cov-2-related cases, hospitalizations and deaths. *medRxiv*, 2022. doi: 10.1101/2022.09.23.22280281. URL `https://doi.org/10.1101/2022.09.23.22280281`.

[4] Affan Shoukat, Thomas N Vilches, Seyed M Moghadas, Pratha Sah, Eric C Schneider, Jaimie Shaff, Alexandra Ternier, Dave A Chokshi, and Alison P Galvani. Lives saved and hospitalizations averted by covid-19 vaccination in new york city: a modeling study. *The Lancet Regional Health - Americas*, 5: 100085, 2022. doi: 10.1016/j. URL `https://doi.org/10.1016/j.`

[5] Eric J. Haas, John M. McLaughlin, Farid Khan, Frederick J. Angulo, Emilia Anis, Marc Lipsitch, Shepherd R. Singer, Gabriel Mircus, Nati Brooks, Meir Smaja, Kaijie Pan, Jo Southern, David L. Swerdlow, Luis Jodar, Yeheskel Levy, and Sharon Alroy-Preis. Infections, hospitalisations, and deaths averted via a nationwide vaccination campaign using the pfizer–biontech bnt162b2 mrna covid-19 vaccine in israel: a retrospective surveillance study. *The Lancet Infectious Diseases*, 22:357–366, 3 2022. ISSN 14744457. doi: 10.1016/S1473-3099(21)00566-1.

[6] Molly K. Steele, Alexia Couture, Carrie Reed, Danielle Iuliano, Michael Whitaker, Hannah Fast, Aron J. Hall, Adam Macneil, Betsy Cadwell, Kristin J. Marks, and Benjamin J. Silk. Estimated number of covid-19 infections, hospitalizations, and deaths prevented among vaccinated persons in the us, december 2020 to september 2021. *JAMA Network Open*, 5:E2220385, 7 2022. ISSN 25743805. doi: 10.1001/jamanetworkopen.2022.20385.

[7] Sam Moore, Edward M. Hill, Louise Dyson, Michael J. Tildesley, and Matt J. Keeling. Retrospectively modeling the effects of increased global vaccine sharing on the covid-19 pandemic. *Nature Medicine*, 11 2022. ISSN 1546170X. doi: 10.1038/s41591-022-02064-y.

[8] Maite Aubry, Noémie Maset, Lloyd Chapman, Aurélie Simon, Sophie Olivier, Raphaëlle Bos, Kiyojiken Chung, Iotefa Teiti, Adam Kucharski, Henri-Pierre Mallet, and Van-Mai Cao-Lormeau. Seroprevalence of sars-cov-2 antibodies in french polynesia and perspective for vaccine strategies. *Preprints*, 2022. doi: 10.20944/preprints202212.0386.v1.

[9] The Economist. The pandemic's true death toll, 2022. URL `https://www.economist.com/graphic-detail/coronavirus-excess-deaths-estimates`.

[10] Charles Whittaker, Patrick G.T. Walker, Mervat Alhaffar, Arran Hamlet, Bimandra A. Djaafara, Azra Ghani, Neil Ferguson, Maysoon Dahab, Francesco Checchi, and Oliver J. Watson. Under-reporting of deaths limits our understanding of true burden of covid-19. *The BMJ*, 375, 10 2021. ISSN 17561833. doi: 10.1136/bmj.n2239.

[11] Rosanna C. Barnard, Nicholas G. Davies, James D. Munday, Rachel Lowe, Gwenan M. Knight, Quentin J. Leclerc, Damien C. Tully, David Hodgson, Rachael Pung, Joel Hellewell, Mihaly Koltai, David Simons, Kaja Abbas, Adam J. Kucharski, Simon R. Procter, Frank G. Sandmann, Carl A.B. Pearson, Kiesha Prem, Alicia Showering, Sophie R. Meakin, Kathleen O'Reilly, Ciara V. McCarthy, Matthew Quaife, Kerry L.M. Wong, Yalda Jafari, Arminder K. Deol, Rein M.G.J. Houben, Charlie Diamond, Thibaut Jombart, C. Julian Villabona-Arenas, William Waites, Rosalind M. Eggo, Akira

Endo, Hamish P. Gibbs, Petra Klepac, Jack Williams, Billy J. Quilty, Oliver Brady, Jon C. Emery, Katherine E. Atkins, Lloyd A.C. Chapman, Katharine Sherratt, Sam Abbott, Nikos I. Bosse, Paul Mee, Sebastian Funk, Jiayao Lei, Yang Liu, Stefan Flasche, James W. Rudge, Fiona Yueqian Sun, Graham Medley, Timothy W. Russell, Amy Gimma, Stéphane Hué, Christopher I. Jarvis, Emilie Finch, Samuel Clifford, Mark Jit, and W. John Edmunds. Modelling the medium-term dynamics of sars-cov-2 transmission in england in the omicron era. *Nature Communications*, 13, 12 2022. ISSN 20411723. doi: 10.1038/s41467-022-32404-y.

[12] Ministère de la Santé en Charge de la Prévention. Bulletin ÉpidÉmiologique hebdomadaire covid-19 polynÉsie franÇaise-n°115, 2022.

[13] Ministère de la Santé en Charge de la Prévention. Bulletin ÉpidÉmiologique hebdomadaire covid-19 polynÉsie franÇaise-n°116, 2022.

[14] Institut de la Statistique de la Polynésie française. Points etudes et bilans de la polynésie française, 2021. URL `https://www.insee.fr/fr/information/4190491`.

[15] Frederik Plesner Lyngse, Carsten Thure Kirkeby, Matthew Denwood, Lasse Engbo Christiansen, Kåre Mølbak, Camilla Holten Møller, Robert Leo Skov, Tyra Grove Krause, Morten Rasmussen, Raphael Niklaus Sieber, Thor Bech Johannesen, Troels Lillebaek, Jannik Fonager, Anders Fomsgaard, Frederik Trier Møller, Marc Stegger, Maria Overvad, Katja Spiess, and Laust Hvas Mortensen. Household transmission of sars-cov-2 omicron variant of concern subvariants ba.1 and ba.2 in denmark. *Nature Communications*, 13, 12 2022. ISSN 20411723. doi: 10.1038/s41467-022-33498-0.

[16] Daichi Yamasoba, Izumi Kimura, Hesham Nasser, Yuhei Morioka, Naganori Nao, Jumpei Ito, Keiya Uriu, Masumi Tsuda, Jiri Zahradnik, Kotaro Shirakawa, Rigel Suzuki, Mai Kishimoto, Yusuke Kosugi, Kouji Kobiyama, Teppei Hara, Mako Toyoda, Yuri L. Tanaka, Erika P. Butlertanaka, Ryo Shimizu, Hayato Ito, Lei Wang, Yoshitaka Oda, Yasuko Orba, Michihito Sasaki, Kayoko Nagata, Kumiko Yoshimatsu, Hiroyuki Asakura, Mami Nagashima, Kenji Sadamasu, Kazuhisa Yoshimura, Jin Kuramochi, Motoaki Seki, Ryoji Fujiki, Atsushi Kaneda, Tadanaga Shimada, Taka aki Nakada, Seiichiro Sakao, Takuji Suzuki, Takamasa Ueno, Akifumi Takaori-Kondo, Ken J. Ishii, Gideon Schreiber, Hirofumi Sawa, Akatsuki Saito, Takashi Irie, Shinya Tanaka, Keita Matsuno, Takasuke Fukuhara, Terumasa Ikeda, and Kei Sato. Virological characteristics of the sars-cov-2 omicron ba.2 spike. *Cell*, 185:2103–2115.e19, 6 2022. ISSN 10974172. doi: 10.1016/j.cell.2022.04.035.

[17] Kimihito Ito, Chayada Piantham, and Hiroshi Nishiura. Estimating relative generation times and reproduction numbers of omicron ba.1 and ba.2 with respect to delta variant in denmark. *Mathematical Biosciences and Engineering*, 19:9005–9017, 2022. ISSN 15510018. doi: 10.3934/mbe.2022418.

[18] Antonio Lentini, Antonio Pereira, Ola Winqvist, and Björn Reinius. Monitoring of the sars-cov-2 omicron ba.1/ba.2 lineage transition in the swedish population reveals increased viral rna levels in ba.2 cases. *Med*, 3:636–643.e4, 9 2022. ISSN 26666340. doi: 10.1016/j.medj.2022.07.007.

[19] United Nations Department of Economic and Social Affairs Population Division. World population prospects, 2019. URL `https://population.un.org/wpp/Download/Archive/Standard/`.

[20] Raphael Sonabend, Lilith K. Whittles, Natsuko Imai, Pablo N. Perez-Guzman, Edward S. Knock, Thomas Rawson, Katy A.M. Gaythorpe, Bimandra A. Djaafara, Wes Hinsley, Richard G. FitzJohn, John A. Lees, Divya Thekke Kanapram, Erik M. Volz, Azra C. Ghani, Neil M. Ferguson, Marc Baguelin, and Anne Cori. Non-pharmaceutical interventions, vaccination, and the sars-cov-2 delta variant in england: a mathematical modelling study. *The Lancet*, 398:1825–1835, 11 2021. ISSN 1474547X. doi: 10.1016/S0140-6736(21)02276-5.

[21] Julia Stowe, Nick Andrews, Freja Kirsebom, Mary Ramsay, and Jamie Lopez Bernal. Effectiveness of covid-19 vaccines against omicron and delta hospitalisation, a test negative case-control study. *Nature Communications*, 13, 12 2022. ISSN 20411723. doi: 10.1038/s41467-022-33378-7.

[22] Nick Andrews, Elise Tessier, Julia Stowe, Charlotte Gower, Freja Kirsebom, Ruth Simmons, Eileen Gallagher, Simon Thelwall, Natalie Groves, Gavin Dabrera, Richard Myers, Colin N.J. Campbell, Gayatri Amirthalingam, Matt Edmunds, Maria Zambon, Kevin Brown, Susan Hopkins, Meera Chand, Shamez N. Ladhani, Mary Ramsay, and Jamie Lopez Bernal. Duration of protection against mild and severe disease by covid-19 vaccines. *New England Journal of Medicine*, 386:340–350, 1 2022. ISSN 0028-4793. doi: 10.1056/nejmoa2115481.

[23] Ross J. Harris, Heather J. Whitaker, Nick J. Andrews, Felicity Aiano, Zahin Amin-Chowdhury, Jessica Flood, Ray Borrow, Ezra Linley, Shazaad Ahmad, Lorraine Stapley, Bassam Hallis, Gayatri Amirthalingam, Katja Höschler, Ben Parker, Alex Horsley, Timothy J.G. Brooks, Kevin E. Brown, Mary E. Ramsay, and Shamez N. Ladhani. Serological surveillance of sars-cov-2: Six-month trends and antibody response in a cohort of public health workers. *Journal of Infection*, 82:162–169, 5 2021. ISSN 15322742. doi: 10.1016/j.jinf.2021.03.015.

[24] Kiesha Prem, Kevin van Zandvoort, Petra Klepac, Rosalind M. Eggo, Nicholas G. Davies, Alex R. Cook, and Mark Jit. Projecting contact matrices in 177 geographical regions: An update and comparison with empirical data for the covid-19 era, 7 2021. ISSN 15537358.

[25] Nicholas G. Davies, Sam Abbott, Rosanna C. Barnard, Christopher I. Jarvis, Adam J. Kucharski, James D. Munday, Carl A. B. Pearson, Timothy W. Russell, Damien C. Tully, Alex D. Washburne, Tom Wenseleers, Amy Gimma, William Waites, Kerry L. M. Wong, Kevin van Zandvoort, Justin D. Silverman, Karla Diaz-Ordaz, Ruth Keogh, Rosalind M. Eggo, Sebastian Funk, Mark Jit, Katherine E. Atkins, and W. John Edmunds. Estimated transmissibility and impact of sars-cov-2 lineage b.1.1.7 in england. *Science*, 372, 4 2021. ISSN 0036-8075. doi: 10.1126/science.abg3055. URL `https://www.science.org/doi/10.1126/science.abg3055`.

[26] Edward S Knock, Lilith K Whittles, John A Lees, Pablo N Perez-Guzman, Robert Verity, Richard G FitzJohn, Katy A M Gaythorpe, Natsuko Imai, Wes Hinsley, Lucy C Okell, Alicia Rosello, Nikolas Kantas, Caroline E Walters, Sangeeta Bhatia, Oliver J Watson, Charlie Whittaker, Lorenzo Cattarino, Adhiratha Boonyasiri, Bimandra A Djaafara, Keith Fraser, Han Fu, Haowei Wang, Xiaoyue Xi, Christl A Donnelly, Elita Jauneikaite, Daniel J Laydon, Peter J White, Azra C Ghani, Neil M Ferguson, Anne Cori, and Marc Baguelin. Key epidemiological drivers and impact of interventions in the 2020 sars-cov-2 epidemic in england, 2021. URL `https://www.science.org`.

[27] Henrik Salje, Cécile Tran Kiem, Noémie Lefrancq, Noémie Courtejoie, Paolo Bosetti, Juliette Paireau, Alessio Andronico, Nathanaël Hozé, Jehanne Richet, Claire Lise Dubost, Yann Le Strat, Justin Lessler, Daniel Levy-Bruhl, Arnaud Fontanet, Lulla Opatowski, Pierre Yves Boelle, and Simon Cauchemez. Estimating the burden of sars-cov-2 in france. *Science*, 369:208–211, 2020. ISSN 10959203. doi: 10.1126/science.abc3517.

[28] Aziz Sheikh, Jim McMenamin, Bob Taylor, and Chris Robertson. Sars-cov-2 delta voc in scotland: demographics, risk of hospital admission, and vaccine effectiveness, 6 2021. ISSN 1474547X.

[29] Nicholas G. Davies, Christopher I. Jarvis, Kevin van Zandvoort, Samuel Clifford, Fiona Yueqian Sun, Sebastian Funk, Graham Medley, Yalda Jafari, Sophie R. Meakin, Rachel Lowe, Matthew Quaife, Naomi R. Waterlow, Rosalind M. Eggo, Jiayao Lei, Mihaly Koltai, Fabienne Krauer, Damien C. Tully, James D. Munday, Alicia Showering, Anna M. Foss, Kiesha Prem, Stefan Flasche, Adam J. Kucharski, Sam Abbott, Billy J. Quilty, Thibaut Jombart, Alicia Rosello, Gwenan M. Knight, Mark Jit, Yang Liu, Jack Williams, Joel Hellewell, Kathleen O'Reilly, Yung Wai Desmond Chan, Timothy W. Russell, Simon R. Procter, Akira Endo, Emily S. Nightingale, Nikos I. Bosse, C. Julian Villabona-Arenas, Frank G. Sandmann, Amy Gimma, Kaja Abbas, William Waites, Katherine E. Atkins, Rosanna C. Barnard, Petra Klepac, Hamish P. Gibbs, Carl A.B. Pearson, Oliver Brady, W. John Edmunds, Nicholas P. Jewell, Karla Diaz-Ordaz, and Ruth H. Keogh. Increased mortality in community-tested cases of sars-cov-2 lineage b.1.1.7. *Nature 2021 593:7858*, 593:270–274, 3 2021. ISSN 1476-4687. doi: 10.1038/s41586-021-03426-1. URL `https://www.nature.com/articles/s41586-021-03426-1`.

[30] Tommy Nyberg, Neil M. Ferguson, Sophie G. Nash, Harriet H. Webster, Seth Flaxman, Nick Andrews, Wes Hinsley, Jamie Lopez Bernal, Meaghan Kall, Samir Bhatt, Paula Blomquist, Asad Zaidi, Erik Volz, Nurin Abdul Aziz, Katie Harman, Sebastian Funk, Sam Abbott, Jamie Lopez Bernal, Nurin Abdul Aziz, Russell Hope, Andre Charlett, Meera Chand, Azra C. Ghani, Shaun R. Seaman, Gavin Dabrera, Daniela De Angelis, Anne M. Presanis, and Simon Thelwall. Comparative analysis of the risks of hospitalisation and death associated with sars-cov-2 omicron (b.1.1.529) and delta (b.1.617.2) variants in england: a cohort study. *The Lancet*, 399:1303–1312, 4 2022. ISSN 1474547X. doi: 10.1016/S0140-6736(22)00462-7.

[31] Nicholas F Brazeau, Robert Verity, Sara Jenks, Han Fu, Charles Whittaker, Peter Winskill, Ilaria Dorigatti, Patrick G T Walker, Steven Riley, Ricardo P Schnekenberg, Henrique Hoeltgebaum, Thomas A Mellan, Swapnil Mishra, H Juliette, T Unwin, Oliver J Watson, Zulma M Cucunubá, Marc Baguelin, Lilith Whittles, Samir Bhatt, Azra C Ghani, Neil M Ferguson, and Lucy C Okell. Estimating the covid-19 infection fatality ratio accounting for seroreversion using statistical modelling. *Communications Medicine 2022 2:1*, 2:1–13, 5 2022. ISSN 2730-664X. doi: 10.1038/s43856-022-00106-7. URL `https://www.nature.com/articles/s43856-022-00106-7`.

[32] Nicholas G. Davies, Petra Klepac, Yang Liu, Kiesha Prem, Mark Jit, and Rosalind M. Eggo. Age-dependent effects in the transmission and control of covid-19 epidemics. *Nature Medicine*, 26, 2020. ISSN 1078-8956. doi: 10.1038/s41591-020-0962-9.

[33] Simon E.F. Spencer. Accelerating adaptation in the adaptive metropolis–hastings random walk algorithm. *Australian and New Zealand Journal of Statistics*, 63:468–484, 9 2021. ISSN 1467842X. doi: 10.1111/anzs.12344.

[34] Richard G. FitzJohn, Edward S. Knock, Lilith K. Whittles, Pablo N. Perez-Guzman, Sangeeta Bhatia, Fernando Guntoro, Oliver J. Watson, Charles Whittaker, Neil M. Ferguson, Anne Cori, Marc Baguelin, and John A. Lees. Reproducible parallel inference and simulation of stochastic state space models using odin, dust, and mcstate. *Wellcome Open Research*, 5:288, 12 2021. doi: 10.12688/wellcomeopenres.16466.1.

[35] Rich FitzJohn, Alex Hill, and John Lees. odin: Ode generation and integration, 2022. URL `https://github.com/mrc-ide/odin`. R package version 1.3.2.

[36] Rich FitzJohn. dust: Iterate multiple realisations of stochastic models, 2022. URL `https://github.com/mrc-ide/odin`. R package version 0.11.24.

[37] Rich FitzJohn, Alex Hill, and John Lees. odin.dust: Compile odin to dust, 2022. URL `https://github.com/mrc-ide/odin.dust`. R package version 0.2.16.

[38] Marc Baguelin, Edward Knock, Lilith Whittles, Rich FitzJohn, John Lees, Anne Cori, Pablo Perez-Guzman, Raphael Sonabend, and Yasin Elmaci. sircovid: Sir model for covid-19, 2022. URL `https://github.com/mrc-ide/sircovid`. R package version 0.12.29.

Acknowledgements

We would like to thank Rich Fitzjohn of the MRC Centre for Global Infectious Disease Analaysis at Imperial College for help with the `R` package `mcstate`.